Joint Transmit Waveform and Receive Filter Design for Dual-Functional Radar-Communication Systems

Rang Liu†, Ming Li†*, Qian Liu†, and A. Lee Swindlehurst‡
†Dalian University of Technology, Dalian, Liaoning 116024, China
E-mail: liurang@mail.dlut.edu.cn, {mli, qianliu}@dlut.edu.cn
‡University of California, Irvine, CA 92697, USA
E-mail: swindle@uci.edu

ICC 2022 - IEEE International Conference on Communications | 978-1-5386-8347-7/22/$31.00 ©2022 IEEE | DOI: 10.1109/ICC45855.2022.9838990

***Abstract*—Space-time adaptive processing (STAP) is an effective method for multi-input multi-output (MIMO) radar systems to identify moving targets in the presence of multiple interferers. The idea of joint optimization in both spatial and temporal domains for radar detection is consistent with the symbol-level precoding (SLP) technique for MIMO communication systems, that optimizes the transmit waveform according to instantaneous transmitted symbols. Therefore, in this paper we combine STAP and constructive interference (CI)-based SLP techniques to realize dual-functional radar-communication (DFRC). The radar output signal-to-interference-plus-noise ratio (SINR) is maximized by jointly optimizing the transmit waveform and receive filter, while satisfying the communication quality-of-service (QoS) constraints and the constant modulus power constraint. An efficient algorithm based on majorization-minimization (MM) and nonlinear equality constrained alternative direction method of multipliers (neADMM) methods is proposed to solve the non-convex optimization problem. Simulation results verify the effectiveness of the proposed DFRC scheme and the associate algorithm.**

***Index Terms*—Dual-functional radar-communication (DFRC), space-time adaptive processing (STAP), symbol-level precoding (SLP), multi-input multi-output (MIMO).**

I. Introduction

Dual-functional radar-communication (DFRC) is regarded as a promising solution to tackle the growing spectrum congestion problem [1]. DFRC systems simultaneously perform target detection and information transmission using the same transmit waveforms from a given platform, which greatly reduces total system cost and hardware complexity. Meanwhile, multi-input multi-output (MIMO) architectures have been widely employed to implement DFRC for improving the spatial-domain waveform diversity. Since the radar and communication functionalities inevitably have conflicting requirements, the waveform design is a crucial problem in pursuing a better performance trade-off [2].

* Corresponding author.

This work is supported in part by the National Natural Science Foundation of China (Grant No. 61971088, 62071083, U1808206, and U1908214), in part by the Natural Science Foundation of Liaoning Province (Grant No. 2020-MS-108), in part by the Fundamental Research Funds for the Central Universities (Grant No. DUT20GJ214 and DUT21GJ208), in part by Dalian Science and Technology Innovation Project (Grant No. 2020JJ25CY001), and in part by the U.S. National Science Foundation under grant CCF-2008714.

Various radar functionality metrics, e.g., the Cramér-Rao bound, the mutual information, the transmit beampattern mean squared error, the waveform covariance similarity, etc., have been considered for waveform designs in MIMO DFRC systems [3]-[5]. However, most existing research has focused on designing the second-order statistics of the transmit waveform, which can only provide limited degrees of freedom (DoFs) in the spatial domain. Moreover, an overly simplified radar sensing environment, in which the target is fixed and there is no clutter or jamming signals, is usually assumed in the prior literature. Therefore, the target detection performance of these designs may not be satisfactory, and may even be unacceptable in a hostile radar sensing environment.

Space-time adaptive processing (STAP) is an effective technique for target detection and clutter suppression, and has been widely applied in airborne surveillance radar systems [6]-[10]. With estimated or prior information about the clutter and interference, STAP directly optimizes spatial-temporal transmit waveforms, rather than their second-order statistics, to maximize the output signal-to-interference-plus-noise ratio (SINR). Since the waveform optimization utilizes the DoFs in both the spatial and temporal domains, the performance of identifying a moving target in the presence of strong clutter over widely spread ranges and angular regions is significantly improved.

Similar to STAP which optimizes the transmit waveforms to improve radar functionality, symbol-level precoding (SLP) also exploits available DoFs in both the spatial and temporal domains to improve communications performance. In particular, SLP designs the transmit precoder in each time slot (i.e., the transmit waveform samples) based on the specific transmitted symbols themselves rather than their second-order statistics [11]-[13]. The advantages of SLP make it a promising technique to consider for DFRC systems in which the transmit waveform used for radar target detection simultaneously carries wireless communications. The transmit waveform can be designed to create constructive interference (CI) that converts harmful multi-user interference (MUI) into useful signal energy to improve the communication quality-of-service (QoS), and to provide an increased SINR for radar detection.

Motivated by the above discussion, in this paper we utilize

STAP and CI-based SLP techniques for implementing DFRC to combine their advantages for both radar and communication functionalities. In particular, we consider a multi-antenna base station (BS) that simultaneously detects a target in the presence of multiple sources of clutter and transfers information symbols to multiple single-antenna users. The transmit waveform and receive filter of the BS are jointly optimized to maximize the radar output SINR under communication QoS and constant modulus power constraints. In order to efficiently solve this non-convex optimization problem, we first employ the majorization-minimization (MM) method and derive a more tractable surrogate function, and then exploit the novel nonlinear equality constrained alternative direction method of multipliers (neADMM) method to handle the constant modulus power constraint after introducing an auxiliary variable. Finally, efficient algorithms and derivations are developed for obtaining the optimal solution to each sub-problem. Simulation results illustrate the effectiveness of the proposed algorithm, and verify the advantages of utilizing STAP and CI-based SLP techniques to implement DFRC.

II. System Model and Problem Formulation

A. System Model

Consider a colocated narrowband DFRC system, where a BS is equipped with N_t transmit antennas and N_r receive antennas arranged as uniform linear arrays (ULAs) with half-wavelength spacing. The BS aims to detect a target in the presence of K strong clutter returns and simultaneously provide downlink wireless communication services to K_u single-antenna users. In order to achieve better performance in target detection and clutter suppression, the BS utilizes the STAP technique to design transmit waveforms in both the spatial and temporal domains. Meanwhile, in order to simultaneously realize communication functionality, the information symbols are carried by transmit waveforms using the CI-based SLP approach for better communication QoS.

We assume that the radar is interrogating the range-angle position (r_0, θ_0) for a target in the presence of K point-like clutter sources located at $(r_k, \theta_k),\ k = 1, \ldots, K$. The range and angle domains are divided into N and L discrete bins respectively indexed as $r_k \in \{0, \ldots, N\}$ and $\theta_k \in \{0, \ldots, L\} \times \frac{2\pi}{L+1},\ \theta_k \neq \theta_0$. The number of range bins N corresponds to the number of samples collected per radar pulse. It is assumed that the location of the clutter sources is known at the BS based on environmental databases or previous adaptive estimation results. The origin of the range coordinates is set at the target range, so that $r_0 = 0$.

Let $\mathbf{x}[n] \triangleq [x_1[n], \ldots, x_{N_\mathrm{t}}[n]]^T$, $n = 1, \ldots, N$, be the n-th sample of the waveform transmitted from the N_t antennas. Unlike prior work, we assume that the BS optimizes each instantaneous waveform sample $\mathbf{x}[n]$ for target detection rather than its second-order statistics. The baseband signals at the receive antennas of the BS can be written as

$$\mathbf{y}[n] = \alpha_0 \mathbf{a}_\mathrm{r}(\theta_0)\mathbf{a}_\mathrm{t}^T(\theta_0)\mathbf{x}[n]e^{\jmath 2\pi(n-1)\nu_0} + \mathbf{c}[n] + \mathbf{z}[n], \quad (1)$$

where α_0 represents the target radar cross section (RCS) with $\mathbb{E}\{|\alpha_0|^2\} = \sigma_0^2$ and ν_0 is the Doppler frequency of the target. The vectors $\mathbf{a}_\mathrm{t}(\theta)$ and $\mathbf{a}_\mathrm{r}(\theta)$ are the steering vectors for the transmit and receive signals at angle θ, respectively:

$$\mathbf{a}_\mathrm{t}(\theta) = \frac{1}{\sqrt{N_\mathrm{t}}}\left[e^{-\jmath\pi 0 \sin\theta}, \ldots, e^{-\jmath\pi(N_\mathrm{t}-1)\sin\theta}\right]^T. \quad (2)$$

The vector $\mathbf{a}_\mathrm{r}(\theta)$ is defined similarly. The signal $\mathbf{c}[n]$ represents the contribution from the K clutter points, and will depend on the transmitted signal:

$$\mathbf{c}[n] = \sum_{k=1}^{K} \alpha_k \mathbf{a}_\mathrm{r}(\theta_k)\mathbf{a}_\mathrm{t}^T(\theta_k)\mathbf{x}[n - r_k]e^{\jmath 2\pi(n-1)\nu_k}, \quad (3)$$

where α_k is the complex amplitude of the k-th clutter reflection with $\mathbb{E}\{|\alpha_k|^2\} = \sigma_k^2$, and ν_k is the corresponding Doppler frequency. For simplicity, in this study we assume that both the target and clutter are slowly-moving and set the Doppler frequencies as zero, i.e., $\nu_0 = \nu_k = 0,\ \forall k$. Finally, the signal $\mathbf{z}[n] \sim \mathcal{CN}(0, \sigma_\mathrm{z}^2\mathbf{I})$ denotes the additive white Gaussian noise (AWGN) at the receive antennas.

For conciseness, we define $\mathbf{y} \triangleq [\mathbf{y}^T[1], \ldots, \mathbf{y}^T[N]]^T$, $\mathbf{x} \triangleq [\mathbf{x}^T[1], \ldots, \mathbf{x}^T[N]]^T$, and $\mathbf{z} \triangleq [\mathbf{z}^T[1], \ldots, \mathbf{z}^T[N]]^T$. Then, the received signals can be re-written as

$$\mathbf{y} = \alpha_0\mathbf{A}_0\mathbf{x} + \sum_{k=1}^{K}\alpha_k\mathbf{A}_k\mathbf{x} + \mathbf{z}, \quad (4)$$

where $\mathbf{A}_k$ is related to the range-angle position (r_k, θ_k), $\mathbf{A}_k \triangleq [\mathbf{I} \otimes (\mathbf{a}_\mathrm{r}(\theta_k)\mathbf{a}_\mathrm{t}^T(\theta_k))]\mathbf{J}_{r_k}$, $k = 0, 1, \ldots, K$, and the shift matrix $\mathbf{J}_{r_k} \in \mathbb{R}^{NN_\mathrm{t} \times NN_\mathrm{t}}$ is defined by

$$\mathbf{J}_{r_k}(i,j) = \begin{cases} 1, & i - j = N_\mathrm{t} r_k, \\ 0, & \text{otherwise}. \end{cases} \quad (5)$$

Denote $\mathbf{w} \in \mathbb{C}^{NN_\mathrm{r}}$ as the linear space-time receive filter whose output can be expressed as

$$r = \mathbf{w}^H\mathbf{y} = \alpha_0\mathbf{w}^H\mathbf{A}_0\mathbf{x} + \mathbf{w}^H\sum_{k=1}^{K}\alpha_k\mathbf{A}_k\mathbf{x} + \mathbf{w}^H\mathbf{z}. \quad (6)$$

Thus, the radar output SINR is given by

$$\gamma = \frac{\sigma_0^2|\mathbf{w}^H\mathbf{A}_0\mathbf{x}|^2}{\mathbf{w}^H\left[\sum_{k=1}^{K}\sigma_k^2\mathbf{A}_k\mathbf{x}\mathbf{x}^H\mathbf{A}_k^H\right]\mathbf{w} + \sigma_\mathrm{z}^2\mathbf{w}^H\mathbf{w}}. \quad (7)$$

Since the target detection probability is generally monotonically increasing with the radar output SINR under Gaussian noise, the joint transmit waveform and receive filter design problem from the radar perspective aims to maximize the radar output SINR (7). Since constant modulus waveforms are usually desired in practical radar systems due to hardware requirements, each element of the transmit waveform $\mathbf{x}$ should satisfy

$$|x_m| = \sqrt{P/N_\mathrm{t}}, \quad \forall m = 1, \ldots, NN_\mathrm{t}, \quad (8)$$

where P is the total available transmit power.

In addition to its radar function, the BS also attempts to deliver information symbols to K_u users using the same transmit waveform. In particular, denote the symbol vector to be transmitted at time n as $\mathbf{s}[n] \triangleq [s_1[n], \ldots, s_{K_\mathrm{u}}[n]]^T$, where each symbol is assumed to be independently selected from an Ω-phase shift keying (PSK) constellation. Each waveform

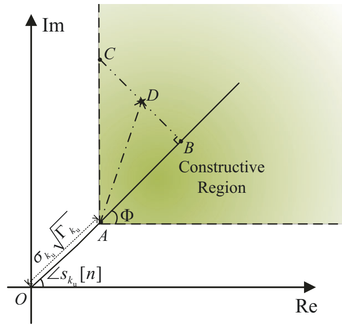

Fig. 1. CI-based SLP for QPSK constellation.

sample $\mathbf{x}[n]$ must be designed to carry the K_u different information symbols in $\mathbf{s}[n]$. The received signal at the k_u-th user can be expressed as

$$r_{k_\mathrm{u}}[n] = \mathbf{h}_{k_\mathrm{u}}^H \mathbf{x}[n] + n_{k_\mathrm{u}}[n], \tag{9}$$

where $\mathbf{h}_{k_\mathrm{u}} \in \mathbb{C}^{N_\mathrm{t}}$ represents the Rayleigh fading channel from the BS to the k_u-th user, and $n_{k_\mathrm{u}}[n] \sim \mathcal{CN}(0, \sigma_{k_\mathrm{u}}^2)$ is AWGN at the k_u-th user. The nonlinear mapping from $\mathbf{s}[n]$ to $\mathbf{x}[n]$ is achieved by the CI-based SLP design as presented below.

Without loss of generality, we take quadrature-PSK (QPSK) constellation (i.e., $\Omega = 4$) as an example to illustrate the CI-based SLP approach as shown in Fig. 1, where $\Phi = \pi/\Omega$ is half of the angular range of the decision regions. Fig. 1 shows the case where the desired symbol of the k_u-th user is $(1/\sqrt{2}, \jmath/\sqrt{2})$, whose decision boundaries are the positive halves of x and y axes. Point D denotes the received noise-free signal $\widetilde{r}_{k_\mathrm{u}}[n] = \mathbf{h}_{k_\mathrm{u}}^H \mathbf{x}[n]$. Unlike conventional block-level precoding approaches aiming to eliminate MUI, the CI-based SLP approach attempts to exploit known symbol information to convert MUI into helpful components that enhance the communication QoS. In particular, let Γ_{k_u} be the QoS requirement of the k_u-th user. If the MUI is entirely eliminated, the received noise-free signal should be at point A to satisfy $\widetilde{r}_{k_\mathrm{u}}[n] = \sigma_{k_\mathrm{u}} \sqrt{\Gamma_{k_\mathrm{u}}} s_{k_\mathrm{u}}[n]$, i.e., $\left|\widetilde{r}_{k_\mathrm{u}}[n]\right|^2 / \sigma_{k_\mathrm{u}}^2 = \Gamma_{k_\mathrm{u}}$. However, MUI in a CI-based SLP system pushes the received noise-free signal deeper into the corresponding constructive (green) region, where the QoS requirement Γ_{k_u} is guaranteed and the distance between the received noise-free signal and its decision boundaries is further enlarged. Thus, better QoS is achieved using the CI-based SLP approach.

The relationship governing the definition of the constructive region can be geometrically expressed as $|\overrightarrow{BC}| - |\overrightarrow{BD}| \geq 0$. Due to space limitations, we omit the derivations and recommend the readers to [11]-[13] for details. The QoS constraints that guarantee that the noise-free received signal $\widetilde{r}_{k_\mathrm{u}}[n]$ lies in the constructive region can be expressed as

$$\begin{aligned} &\Re\left\{\mathbf{h}_{k_\mathrm{u}}^H \mathbf{x}[n] e^{-\jmath \angle s_{k_\mathrm{u}}[n]} - \sigma_{k_\mathrm{u}} \sqrt{\Gamma_{k_\mathrm{u}}}\right\} \sin\Phi \\ &\quad - \left|\Im\left\{\mathbf{h}_{k_\mathrm{u}}^H \mathbf{x}[n] e^{-\jmath \angle s_{k_\mathrm{u}}[n]}\right\}\right| \cos\Phi \geq 0, \quad \forall k_\mathrm{u}, \ \forall n. \end{aligned} \tag{10}$$

In order to represent (10) in a compact form, we define

$$\widetilde{\mathbf{h}}_{(2k_\mathrm{u}-2)N+n}^H \triangleq \mathbf{e}_n^T \otimes \mathbf{h}_{k_\mathrm{u}}^H e^{-\jmath \angle s_{k_\mathrm{u}}[n]} (\sin\Phi + e^{-\jmath \frac{\pi}{2}} \cos\Phi), \tag{11a}$$

$$\widetilde{\mathbf{h}}_{(2k_\mathrm{u}-1)N+n}^H \triangleq \mathbf{e}_n^T \otimes \mathbf{h}_{k_\mathrm{u}}^H e^{-\jmath \angle s_{k}[n]} (\sin\Phi - e^{-\jmath \frac{\pi}{2}} \cos\Phi), \tag{11b}$$

$$\gamma_{(2k_\mathrm{u}-2)N+n} = \gamma_{(2k_\mathrm{u}-1)N+n} \triangleq \sigma_{k_\mathrm{u}} \sqrt{\Gamma_{k_\mathrm{u}}} \sin\Phi, \tag{11c}$$

where the vector $\mathbf{e}_n \in \mathbb{R}^N$ has a 1 in position n and zeros elsewhere, and $\otimes$ denotes the Kronecker product. Then, the communication QoS constraints are equivalently re-written as

$$\Re\{\widetilde{\mathbf{h}}_i^H \mathbf{x}\} \geq \gamma_i, \quad \forall i = 1, \ldots, 2K_\mathrm{u}N. \tag{12}$$

B. Problem Formulation

In this paper, we aim to jointly design the transmit waveform $\mathbf{x}$ and the receive filter $\mathbf{w}$ to maximize the output SINR (7), while satisfying the communication QoS requirements (10) and the constant modulus power constraint (8). Therefore, the optimization problem is formulated as

$$\max_{\mathbf{x},\mathbf{w}} \quad \frac{\sigma_0^2 |\mathbf{w}^H \mathbf{A}_0 \mathbf{x}|^2}{\mathbf{w}^H \left[\sum_{k=1}^K \sigma_k^2 \mathbf{A}_k \mathbf{x}\mathbf{x}^H \mathbf{A}_k^H\right] \mathbf{w} + \sigma_\mathrm{z}^2 \mathbf{w}^H \mathbf{w}} \tag{13a}$$

$$\text{s.t.} \quad \Re\{\widetilde{\mathbf{h}}_i^H \mathbf{x}\} \geq \gamma_i, \quad \forall i = 1, \ldots, 2K_\mathrm{u}N, \tag{13b}$$

$$|x_m| = \sqrt{P/N_\mathrm{t}}, \quad \forall m = 1, \ldots, NN_\mathrm{t}. \tag{13c}$$

It can be observed that with a fixed transmit waveform $\mathbf{x}$, the original problem (13) becomes a well-known minimum variance distortionless response (MVDR) problem:

$$\min_{\mathbf{w}} \quad \mathbf{w}^H \Big[\sum_{k=1}^K \sigma_k^2 \mathbf{A}_k \mathbf{x}\mathbf{x}^H \mathbf{A}_k^H + \sigma_\mathrm{z}^2 \mathbf{I}\Big] \mathbf{w} \tag{14a}$$

$$\text{s.t.} \quad \mathbf{w}^H \mathbf{A}_0 \mathbf{x} = 1. \tag{14b}$$

The closed-form optimal solution $\mathbf{w}^\star$ in this case can be easily obtained as

$$\mathbf{w}^\star = \frac{\left[\sum_{k=1}^K \sigma_k^2 \mathbf{A}_k \mathbf{x}\mathbf{x}^H \mathbf{A}_k^H + \sigma_\mathrm{z}^2 \mathbf{I}\right]^{-1} \mathbf{A}_0 \mathbf{x}}{\mathbf{x}^H \mathbf{A}_0^H \left[\sum_{k=1}^K \sigma_k^2 \mathbf{A}_k \mathbf{x}\mathbf{x}^H \mathbf{A}_k^H + \sigma_\mathrm{z}^2 \mathbf{I}\right]^{-1} \mathbf{A}_0 \mathbf{x}}. \tag{15}$$

Substituting $\mathbf{w}^\star$ into the original optimization problem (13) leads to the concentrated transmit waveform design problem:

$$\min_{\mathbf{x}} \quad -\mathbf{x}^H \mathbf{A}_0^H \Big[\sum_{k=1}^K \sigma_k^2 \mathbf{A}_k \mathbf{x}\mathbf{x}^H \mathbf{A}_k^H + \sigma_\mathrm{z}^2 \mathbf{I}\Big]^{-1} \mathbf{A}_0 \mathbf{x} \tag{16a}$$

$$\text{s.t.} \quad \Re\{\widetilde{\mathbf{h}}_i^H \mathbf{x}\} \geq \gamma_i, \quad \forall i, \tag{16b}$$

$$|x_m| = \sqrt{P/N_\mathrm{t}}, \quad \forall m. \tag{16c}$$

Since (16) is a complicated non-convex optimization problem due to the non-convex objective function (16a) and the constant modulus power constraint (16c), a direct solution is very difficult to obtain. In order to tackle these difficulties, in next section we employ MM and neADMM methods to convert problem (16) into two tractable sub-problems and iteratively solve them.

III. Transmit Waveform Design

In order to efficiently handle the complicated non-convex objective function (16a), we utilize the MM method to find a more tractable convex surrogate function that is an approximate local upper-bound of (16a) in each iteration. Defining $f(\mathbf{x}) \triangleq -\mathbf{x}^H \mathbf{A}_0^H \left[\sum_{k=1}^K \sigma_k^2 \mathbf{A}_k \mathbf{x}\mathbf{x}^H \mathbf{A}_k^H + \sigma_\mathrm{z}^2 \mathbf{I}\right]^{-1} \mathbf{A}_0 \mathbf{x}$, the derivation for a surrogate function of $f(\mathbf{x})$ is based on the following lemma [14].

$$
\begin{aligned}
f(\mathbf{x}) \leq \operatorname{Tr}\Big\{\Big[\sum_{k=1}^{K}\sigma_k^2\mathbf{A}_k\mathbf{X}_t^H\mathbf{A}_k^H+\sigma_z^2\mathbf{I}\Big]^{-1}\mathbf{A}_0\mathbf{x}_t\mathbf{x}_t^H\mathbf{A}_0^H\Big[\sum_{k=1}^{K}\sigma_k^2\mathbf{A}_k\mathbf{X}_t^H\mathbf{A}_k^H+\sigma_z^2\mathbf{I}\Big]^{-1}\Big[\sum_{k=1}^{K}\sigma_k^2\mathbf{A}_k\mathbf{X}^H\mathbf{A}_k^H+\sigma_z^2\mathbf{I}\Big]\Big\} \quad (17a)\\
-2\Re\Big\{\mathbf{x}_t^H\mathbf{A}_0^H\Big[\sum_{k=1}^{K}\sigma_k^2\mathbf{A}_k\mathbf{X}_t^H\mathbf{A}_k^H+\sigma_z^2\mathbf{I}\Big]^{-1}\mathbf{A}_0\mathbf{x}\Big\}+\text{const}\\
=\operatorname{Tr}\{\mathbf{D}_t\mathbf{X}\}-\Re\{\mathbf{b}_t^H\mathbf{x}\}+\text{const}. \quad (17b)
\end{aligned}
$$

Lemma 1. *For a positive-definite matrix* $\mathbf{M}$*,* $\mathbf{s}^H\mathbf{M}^{-1}\mathbf{s}$ *is a convex function of* $\mathbf{s}$ *and* $\mathbf{M}$*, and its surrogate function at point* $(\mathbf{s}_t,\mathbf{M}_t)$ *is given by*

$$\mathbf{s}^H\mathbf{M}^{-1}\mathbf{s} \geq 2\Re\{\mathbf{s}_t^H\mathbf{M}_t^{-1}\mathbf{s}\}-Tr\{\mathbf{M}_t^{-1}\mathbf{s}_t\mathbf{s}_t^H\mathbf{M}_t^{-1}\mathbf{M}\}+const,$$

where $Tr\{\mathbf{A}\}$ *indicates the trace of a matrix* $\mathbf{A}$*, and "const" is a constant term that is irrelevant to the variables.*

Inspired by Lemma 1, we define $\mathbf{X}\triangleq\mathbf{x}\mathbf{x}^H$, the affine transformation $\mathbf{s}\triangleq\mathbf{A}_0\mathbf{x}$, and $\mathbf{M}\triangleq\sum_{k=1}^{K}\sigma_k^2\mathbf{A}_k\mathbf{X}\mathbf{A}_k^H+\sigma_z^2\mathbf{I}$. Then, the surrogate function of $f(\mathbf{x})$ can be calculated as (17) presented at the top of this page, where we define

$$\mathbf{b}_t \triangleq 2\mathbf{A}_0^H\Big[\sum_{k=1}^{K}\sigma_k^2\mathbf{A}_k\mathbf{X}_t\mathbf{A}_k^H+\sigma_z^2\mathbf{I}\Big]^{-1}\mathbf{A}_0\mathbf{x}_t, \quad (18a)$$

$$\mathbf{D}_t \triangleq \sum_{k=1}^{K}\sigma_k^2\mathbf{G}_{t,k}^H\mathbf{X}_t\mathbf{G}_{t,k}, \quad (18b)$$

$$\mathbf{G}_{t,k} \triangleq \mathbf{A}_0^H\Big[\sum_{k=1}^{K}\sigma_k^2\mathbf{A}_k\mathbf{X}_t\mathbf{A}_k^H+\sigma_z^2\mathbf{I}\Big]^{-1}\mathbf{A}_k. \quad (18c)$$

Substituting $\mathbf{X}\triangleq\mathbf{x}\mathbf{x}^H$ into (17) and ignoring the constant term, the transmit waveform design problem at point $\mathbf{x}_t$ can be written as

$$
\begin{aligned}
\min_{\mathbf{x}} \quad & \mathbf{x}^H\mathbf{D}_t\mathbf{x}-\Re\{\mathbf{b}_t^H\mathbf{x}\} && (19a)\\
\text{s.t.} \quad & \Re\{\widetilde{\mathbf{h}}_i^H\mathbf{x}\}\geq\gamma_i, \quad \forall i, && (19b)\\
& |x_m|=\sqrt{P/N_\text{t}}, \quad \forall m. && (19c)
\end{aligned}
$$

It can be observed that although the objective function (19a) is continuous and convex, problem (19) is still a non-convex problem due to the constant modulus power constraint (19c). While the classical ADMM method can only handle linear equality constraints, the new neADMM approach [15] can be applied to nonlinear equality constraints such as (19c). Therefore, we develop an neADMM-based method to solve this problem as follows.

We first introduce an auxiliary variable $\mathbf{y}\triangleq[y_1,\ldots,y_{NN_\text{t}}]^T$ to decouple the convex constraint (19b) and the non-convex constraint (19c) with respect to $\mathbf{x}$, and convert (19) to

$$
\begin{aligned}
\min_{\mathbf{x},\mathbf{y}} \quad & \mathbf{x}^H\mathbf{D}_t\mathbf{x}-\Re\{\mathbf{b}_t^H\mathbf{x}\} && (20a)\\
\text{s.t.} \quad & \Re\{\widetilde{\mathbf{h}}_i^H\mathbf{x}\}\geq\gamma_i, \quad \forall i, && (20b)\\
& |x_m|\leq\sqrt{P/N_\text{t}}, \quad \forall m, && (20c)\\
& \mathbf{x}=\mathbf{y}, && (20d)\\
& |y_m|=\sqrt{P/N_\text{t}}, \quad \forall m. && (20e)
\end{aligned}
$$

To accommodate the neADMM framework, we define the feasible region of the inequality constraints (20b) and (20c) as set $\mathcal{C}$, and an indicator function $\mathbb{I}_\mathcal{C}$ associated with $\mathcal{C}$ as

$$\mathbb{I}_\mathcal{C}(\mathbf{x})=\begin{cases}0, & \mathbf{x}\in\mathcal{C},\\ +\infty, & \text{otherwise.}\end{cases} \quad (21)$$

Then, by removing the constraints on $\mathbf{x}$ and adding the feasibility indicator function in the objective, problem (20) is transformed to

$$
\begin{aligned}
\min_{\mathbf{x},\mathbf{y}} \quad & \mathbf{x}^H\mathbf{D}_t\mathbf{x}-\Re\{\mathbf{b}_t^H\mathbf{x}\}+\mathbb{I}_\mathcal{C}(\mathbf{x}) && (22a)\\
\text{s.t.} \quad & \mathbf{x}=\mathbf{y}, && (22b)\\
& |y_m|=\sqrt{P/N_\text{t}}, \quad \forall m, && (22c)
\end{aligned}
$$

whose solution can be obtained by optimizing its augmented Lagrangian (AL) function. Specifically, the AL function of problem (22) is expressed as

$$
\begin{aligned}
&\mathcal{L}(\mathbf{x},\mathbf{y},\boldsymbol{\lambda},\boldsymbol{\mu})\triangleq\mathbf{x}^H\mathbf{D}_t\mathbf{x}-\Re\{\mathbf{b}_t^H\mathbf{x}\}+\mathbb{I}_\mathcal{C}(\mathbf{x})\\
&\quad+\frac{\rho}{2}\|\mathbf{x}-\mathbf{y}+\boldsymbol{\lambda}/\rho\|^2+\frac{\rho}{2}\||\mathbf{y}|-\sqrt{P/N_\text{t}}+\boldsymbol{\mu}/\rho\|^2,
\end{aligned} \quad (23)
$$

where $\rho>0$ is a penalty parameter, $\boldsymbol{\lambda}\in\mathbb{C}^{NN_\text{t}}$ and $\boldsymbol{\mu}\in\mathbb{C}^{NN_\text{t}}$ are dual variables, and $|\cdot|$ is an element-wise absolute value operation. The AL function (23) is a more tractable function with multiple variables, which can be alternately minimized by updating $\mathbf{x}$, $\mathbf{y}$, $\boldsymbol{\lambda}$, and $\boldsymbol{\mu}$ as shown below.

1) ***Update*** $\mathbf{x}$: With given $\mathbf{y}$, $\boldsymbol{\lambda}$ and $\boldsymbol{\mu}$, the optimization problem for updating $\mathbf{x}$ is formulated as

$$\min_{\mathbf{x}} \quad \mathbf{x}^H\mathbf{D}_t\mathbf{x}-\Re\{\mathbf{b}_t^H\mathbf{x}\}+\mathbb{I}_\mathcal{C}(\mathbf{x})+\frac{\rho}{2}\|\mathbf{x}-\mathbf{y}+\boldsymbol{\lambda}/\rho\|^2. \quad (24)$$

According to the definition of $\mathbb{I}_\mathcal{C}(\mathbf{x})$ in (21), problem (24) can be equivalently transformed into a convex second-order cone programming (SOCP) problem:

$$
\begin{aligned}
\min_{\mathbf{x}} \quad & \mathbf{x}^H\mathbf{D}_t\mathbf{x}-\Re\{\mathbf{b}_t^H\mathbf{x}\}+\frac{\rho}{2}\|\mathbf{x}-\mathbf{y}+\boldsymbol{\lambda}/\rho\|^2 && (25a)\\
\text{s.t.} \quad & \Re\{\widetilde{\mathbf{h}}_i^H\mathbf{x}\}\geq\gamma_i, \quad \forall i, && (25b)\\
& |x_m|\leq\sqrt{P/N_\text{t}}, \quad \forall m, && (25c)
\end{aligned}
$$

whose optimal solution can be efficiently obtained by various off-the-shelf algorithms or optimization tools, e.g., CVX.

2) ***Update*** $\mathbf{y}$: With fixed $\mathbf{x}$, $\boldsymbol{\lambda}$ and $\boldsymbol{\mu}$, the optimization problem for updating $\mathbf{y}$ is given by

$$\min_{\mathbf{y}} \quad \frac{\rho}{2}\|\mathbf{x}-\mathbf{y}+\boldsymbol{\lambda}/\rho\|^2+\frac{\rho}{2}\||\mathbf{y}|-\sqrt{P/N_\text{t}}+\boldsymbol{\mu}/\rho\|^2. \quad (26)$$

We observe that problem (26) is a non-convex problem due to the absolute value operation. Fortunately, each element of $\mathbf{y}$ is independent in problem (26). Thus we can equivalently

Algorithm 1 Transmit Waveform Design Algorithm

Input: $\mathbf{A}_0$, $\mathbf{A}_k$, σ_k, $\forall k$, σ_z, $\widetilde{\mathbf{h}}_i$, γ_i, $\forall i$, P, ρ, δ_{th}.
Output: $\mathbf{x}^\star$.

Initialize $\mathbf{x}$, $\mathbf{y}$, $\boldsymbol{\lambda}$, $\boldsymbol{\mu}$, $\delta = \infty$.
while $\delta \geq \delta_{\text{th}}$ **do**
  Update $\mathbf{x}$ by solving (25).
  Update y_m, $\forall m$, by (30).
  Update $\boldsymbol{\lambda}$ by (31a).
  Update $\boldsymbol{\mu}$ by (31b).
  $\delta = \|\mathbf{x} - \mathbf{y}\|^2 + \|\mathbf{y} - \sqrt{P/N_{\text{t}}}\|^2$.
end while
$\mathbf{x}^\star = \mathbf{x}$.

divide (26) into NN_{t} sub-problems. The m-th sub-problem is expressed as

$$\min_{y_m} \quad |y_m - a_m|^2 + \big||y_m| - b_m\big|^2, \tag{27}$$

where $a_m \triangleq x_m + \lambda_m/\rho$ and $b_m \triangleq \sqrt{P/N_{\text{t}}} - \mu_m/\rho$. In order to handle the absolute value function, the objective of (27) is expanded as

$$|y_m - a_m|^2 + \big||y_m| - b_m\big|^2 \tag{28a}$$
$$= 2|y_m|^2 - 2\Re\big\{(a_m^* y_m + b_m^* |y_m|)\big\} + |a_m|^2 + |b_m|^2 \tag{28b}$$
$$= 2|y_m|^2 - 2|y_m|\Re\big\{(a_m^* e^{\jmath\angle y_m} + b_m^*)\big\} + |a_m|^2 + |b_m|^2. \tag{28c}$$

Since $|y_m| \geq 0$, we can easily obtain the optimal angle of y_m as $\angle y_m^\star = \angle a_m$. Substituting $\angle y_m^\star$ into (28c), the optimal amplitude of y_m can be obtained by solving

$$\min_{|y_m|} \quad 2|y_m|^2 - 2|y_m|(|a_m| + \Re\{b_m\}), \tag{29}$$

whose optimal solution is given by $|y_m^\star| = 0.5(|a_m| + \Re\{b_m\})$. Therefore, the optimal solution to problem (27) is

$$y_m^\star = 0.5\big(|a_m| + \Re\{b_m\}\big)e^{\jmath\angle a_m}. \tag{30}$$

3) ***Update $\boldsymbol{\lambda}$ and $\boldsymbol{\mu}$***: After obtaining $\mathbf{x}$ and $\mathbf{y}$, the dual variables are updated by

$$\boldsymbol{\lambda}^\star := \boldsymbol{\lambda} + \rho(\mathbf{x} - \mathbf{y}), \tag{31a}$$
$$\boldsymbol{\mu}^\star := \boldsymbol{\mu} + \rho\big(|\mathbf{y}| - \sqrt{P/N_{\text{t}}}\big). \tag{31b}$$

With above derivations, the transmit waveform design algorithm is straightforward and summarized in Algorithm 1, where δ_{th} is the threshold to judge the convergence and δ is the primal residual. In summary, the transmit waveform $\mathbf{x}$ is obtained by iteratively updating $\mathbf{x}$, $\mathbf{y}$, $\boldsymbol{\lambda}$ and $\boldsymbol{\mu}$ via (25), (30), (31a) and (31b), respectively, until the equality constraints (22b) and (22c) are approximately met. Finally, with the obtained transmit waveform $\mathbf{x}^\star$, the optimal receive filter $\mathbf{w}^\star$ can be calculated by (15).

IV. Simulation Results

In this section, we provide simulation results to show the effectiveness of the proposed joint transmit waveform and receive filter design algorithm. The following settings are assumed throughout our simulations. The BS is equipped with the same number of transmit and receive antennas, denoted by N_{a}. The number of waveform samples for each radar pulse is $N = 20$. The target is located at the range-angle position $(0, 15^\circ)$ with power $\sigma_0^2 = 20$dB. The $K = 3$ clutter sources are respectively located at $(0, -50^\circ)$, $(1, -10^\circ)$, and $(2, 40^\circ)$ with power $\sigma_k^2 = 20$dB, $\forall k$. The noise power is $\sigma_{\text{z}}^2 = 0$dB. The BS is also transmitting QPSK signals to $K_{\text{u}} = 3$ communication users, and the communication noise power is set as $\sigma_{k_{\text{u}}}^2 = -20$dB, $\forall k_{\text{u}}$. The communication QoS for all K_{u} users is the same and is denoted by Γ. The penalty parameter of the neADMM method is chosen as $\rho = 2$.

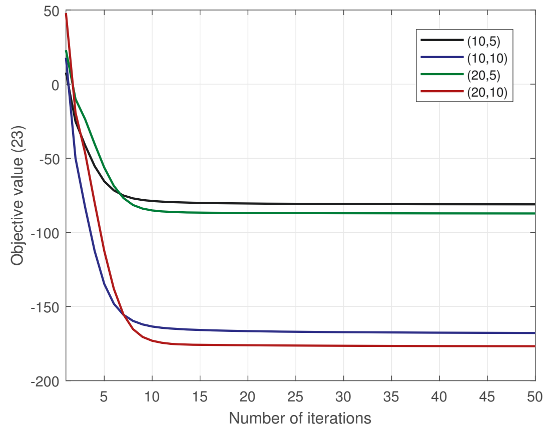

Fig. 2. Convergence illustration ($\Gamma = 10$dB).

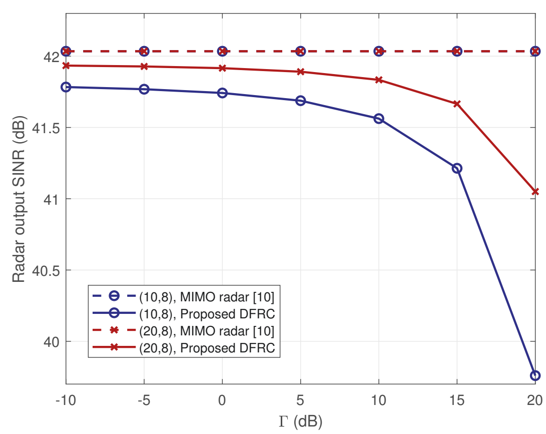

Fig. 3. Radar output SINR versus communication QoS.

We first show the convergence performance of the algorithm for the cases with different transmit powers and different numbers of antennas in Fig. 2, where (x, y) denotes the settings for N_{a} and P. We see that in all cases convergence is achieved within only 20 iterations, and the objective value monotonically decreases with each iteration, consistent with the behavior of the MM method.

The radar output SINR γ versus the communication QoS requirements Γ is shown in Fig. 3. The performance of the MIMO radar scheme in [10] is also plotted as a benchmark. Not surprisingly, the achieved radar output SINR decreases as the communication QoS requirements increase due to the trade-off between target detection performance and wire-

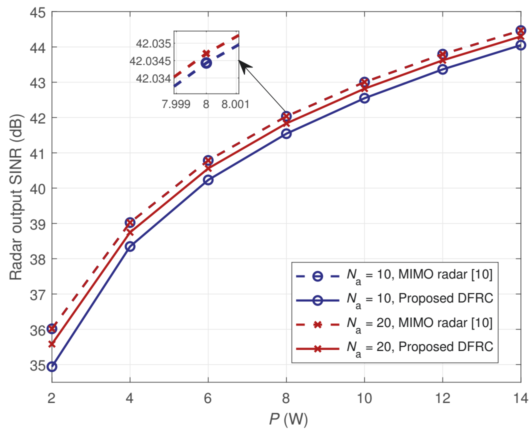

Fig. 4. Radar output SINR versus transmit power P ($\Gamma = 10$dB).

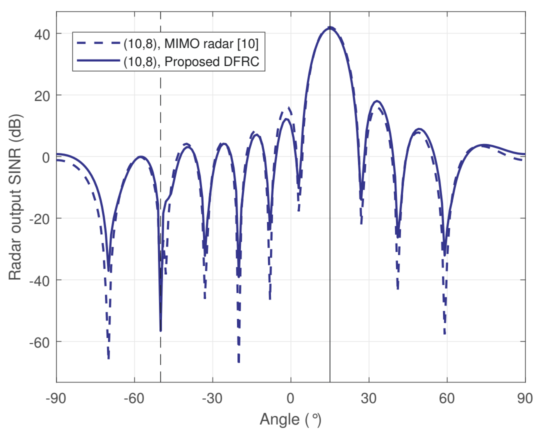

Fig. 5. Radar output SINR at each angle ($\Gamma = 10$dB).

less communication QoS. Additional transmit/receive antennas provide a larger radar output SINR. In addition, it can be seen that an increase in the number of antennas brings a larger performance improvement to the proposed DFRC approach than the conventional MIMO radar scheme. More importantly, we observe that the BS can provide $K_u = 3$ users with a $\Gamma = 10$dB communication QoS at the price of only about 0.5dB in radar performance loss, which confirms the advantages of utilizing STAP and CI-based SLP techniques in DFRC systems. We also illustrate the radar output SINR versus the transmit power P in Fig. 4. It is natural that the radar output SINR increases with the increasing of transmit power for all schemes. Moreover, it can be seen that with the same transmit power, more transmit antennas provide a higher performance gain for the DFRC system than the MIMO radar counterpart, which verifies the advancement of the MIMO architecture for DFRC systems.

Finally, the radar output SINR at each angle is presented in Fig. 5. It can be observed that the achieved radar output SINR of both the conventional MIMO radar and the proposed DFRC approaches reaches its peak value at $\theta = 15°$ and drops to very small values at the angles of the clutter. Moreover, we see that the proposed DFRC algorithm has only a marginal SINR loss for the radar, which ensures satisfactory target angular resolution performance when simultaneously performing communications.

V. Conclusions

In this paper, we investigated joint transmit waveform and receive filter design for DFRC systems. The instantaneous radar output SINR was maximized under a constant modulus power constraint and CI constraints that guarantee the communication QoS is satisfied. An efficient algorithm exploiting MM and neADMM methods was developed to solve the resulting complicated non-convex optimization problem. Simulation examples demonstrated the advantages of utilizing STAP and CI-based SLP techniques to implement DFRC, as well as the effectiveness of the proposed algorithm.

References

[1] L. Zheng, M. Lops, Y. C. Eldar, and X. Wang, "Radar and communication co-existence: An overview," *IEEE Signal Process. Mag.*, vol. 36, no. 5, pp. 85-89, Sep. 2019.

[2] J. A. Zhang, M. L. Rahman, K. Wu, X. Huang, Y. J. Guo, S. Chen, and J. Yuan, "Enabling joint communication and radar sensing in mobile networks - A survey," Jan. 2021. [Online]. Available: https://arxiv.org/abs/2006.07559

[3] F. Liu, C. Masouros, A. Li, H. Sun, and L. Hanzo, "MU-MIMO communications with MIMO radar: From co-existence to joint transmission," *IEEE Trans. Wireless Commun.*, vol. 17, no. 4, pp. 2755-2770, Apr. 2018.

[4] X. Liu, T. Huang, N. Shlezinger, Y. Liu, J. Zhou, and Y. C. Eldar, "Joint transmit beamforming for multiuser MIMO communications and MIMO radar," *IEEE Trans. Signal Process.*, vol. 68, pp. 3929-3944, Jun. 2020.

[5] Z. Cheng, B. Liao, and Z. He, "Hybrid transceiver design for dual-functional radar-communication system," in *Proc. IEEE Sensor Array Multichannel Signal Process. Workshop (SAM)*, Hangzhou, China, Jun. 2020.

[6] J. R. Guerci, *Space-Time Adaptive Processing for Radar*. Norwood, MA, USA: Artech House, 2014.

[7] A. Aubry, A. DeMaio, A. Farina, and M. Wicks, "Knowledge-aided (potentially cognitive) transmit signal and receive filter design in signal dependent clutter," *IEEE Trans. Aerosp. Electron. Syst.*, vol. 49, no. 1, pp. 93-117, Jan. 2013.

[8] G. Cui, H. Li, and M. Rangaswamy, "MIMO radar waveform design with constant modulus and similarity constraints," *IEEE Trans. Signal Process.*, vol. 62, no. 2, pp. 343-353, Jan. 2014.

[9] G. Cui, X. Yu, V. Carotenuto, and L. Kong, "Space-time transmit code and receive filter design for colocated MIMO radar," *IEEE Trans. Signal Process.*, vol. 65, no. 5, pp. 1116-1129, Mar. 2017.

[10] L. Wu, P. Babu, and D. P. Palomar, "Transmit waveform/receive filter design for MIMO radar with multiple waveform constraints," *IEEE Trans. Signal Process.*, vol. 66, no. 6, pp. 1526-1540, Mar. 2018.

[11] M. Alodeh, *et al.*, "Symbol-level and multicast precoding for multiuser multiantenna downlink: A state-of-art, classification, and challenges," *IEEE Commun. Surveys Tut.*, vol. 20, no. 3, pp. 1733-1757, May 2018.

[12] A. Li, *et al.*, "A tutorial on interference exploitation via symbol-level precoding: Overview, state-of-the-art and future directions," *IEEE Commun. Surveys Tut.*, vol. 22, no. 2, pp. 796-839, 2nd quarter 2020.

[13] R. Liu, M. Li, Q. Liu, and A. L. Swindlehurst, "Joint symbol-level precoding and reflecting designs for IRS-enhanced MU-MISO systems," *IEEE Trans. Wireless Commun.*, vol. 20, no. 2, pp. 798-811, Feb. 2021.

[14] Y. Sun, P. Babu, and D. P. Palomar, "Majorization-minimization algorithms in signal processing, communications, and machine learning," *IEEE Trans. Signal Process.*, vol. 65, no. 3, pp. 794-816, Feb. 2017.

[15] Y. Liu, J. Zhao, M. Li, and Q. Wu, "Intelligent reflecting surface aided MISO uplink communication network: Feasibility and power minimization for perfect and imperfect CSI," *IEEE Trans. Commun.*, vol. 69, no. 3, pp. 1975-1989, Mar. 2021.